JAERI-M
9698

# STUDY OF EQUILIBRIUM AND AXISYMMETRIC STABILITY OF DEE-SHAPED PLASMAS IN DOUBLET III

(Doublet-III Experimental Report, 9)

September 1981

H. YOKOMIZO, M. NAGAMI, M. SHIMADA,
N. BROOKS,[*1] R. SERAYDARIAN,[*1] K. SHINYA,[*2]
M. MAENO, H. YOSHIDA, K. IOKI,[*3] S. IZUMI,[*4]
P. ROCK,[*1] N. FUJISAWA and A. KITSUNEZAKI

日本原子力研究所
Japan Atomic Energy Research Institute

この報告書は，日本原子力研究所がJAERI-Mレポートとして，不定期に刊行している研究報告書です．入手，複製などのお問合わせは，日本原子力研究所技術情報部（茨城県那珂郡東海村）あて，お申しこしください．

JAERI-M reports, issued irregularly, describe the results of research works carried out in JAERI. Inquiries about the availability of reports and their reproduction should be addressed to Division of Technical Information, Japan Atomic Energy Research Institute, Tokai-mura, Naka-gun, Ibaraki-ken, Japan.

JAERI-M 9698

# Study of Equilibrium and Axisymmetric Stability of Dee-shaped Plasmas in Doublet III

(Doublet-III Experimental Report, 9)

Hideaki YOKOMIZO, Masayuki NAGAMI, Michiya SHIMADA, N. BROOKS[*1], R. SERAYDARIAN[*1]
Kichiro SHINYA[*2], Masaki MAENO, Hidetoshi YOSHIDA, Kimihiro IOKI[*3]
Shigeru IZUMI[*4], P. ROCK[*1], Noboru FUJISAWA and Akio KITSUNEZAKI

Division of Thermonuclear Fusion Research,
Tokai Research Establishment, JAERI

(Received September 4, 1981)

Stable plasmas with a surface elongation of up to 1.8 have been produced in the upper lobe of the Doublet III vacuum vessel. In plasmas with elongation greater than 1.8, the active feedback control on Doublet III is inadequate to prevent a vertical instability. The growth rate of the vertical instability has been measured at various values of elongation, by disabling the feedback circuit of the vertical position control power supply. These measured growth rates are compared with those predicted from the limited stabilization effect of the passive field-shaping coils. The dee shape is found to be preferable to an elliptical one because its triangularity reduces the absolute value of the field decay index required to produce a given elongation.

Keywords; Doublet-III, D-shaped Cross Section, Elongation, Triangularity, Plasma Position Control

---

This work was performed under a cooperative agreement between the Japan Atomic Energy Research Institute and the United States Department of Energy under DOE Contract No. DE-AT03-80SF11512.

*1) General Atomic Company, San Diego, California, USA.
*2) On leave from Toshiba Electric Company, Kanagawa, Japan.
*3) On leave from Mitsubishi Atomic Power Industry, Saitama, Japan.
*4) On leave from Hitachi Ltd., Ibaraki, Japan.

# ダブレットⅢD形プラズマの平衡と軸対称安定性の研究（ダブレットⅢ実験報告・9）

日本原子力研究所東海研究所大型トカマク開発部
横溝英明・永見正幸・嶋田道也・N. H. BROOKS [*1]
R. P. SERAYDARIAN [*1]・新谷吉郎 [*2]・前野勝樹
吉田英俊・伊尾木公裕 [*3]・出海　滋 [*4]・P. ROCK [*1]
藤沢　登・狐崎晶雄

（1981年9月4日受理）

非円形度1.8までのプラズマをダブレットⅢ装置で安定に制御することができた。装置の制御応答が十分でないため，1.8以上の非円形プラズマは垂直方向に不安定となる。垂直方向の位置不安定を制御している電源を断にすることによって，いろいろな非円形度のプラズマの位置不安定の生長率を測定した。これらの測定値と形状制御コイルがもっているパッシブな安定化効果を考慮した生長率との比較をした。D形の変形は楕円断面に適したものであることが判った。なぜならば，三角度が楕円形を作るのに必要な磁場の曲率指数を減す方向に働くためである。

＊1） General Atomic Company, U. S. A.
＊2） 外来研究員；東京芝浦電気（株）
＊3） 外来研究員；三菱原子力工業（株）
＊4） 外来研究員；日立製作所（株）

Contents



# 目　　次

# 1. INTRODUCTION

For future tokamak reactors, a dee-shaped plasma is believed to have the most advantageous cross-section for achieving high β values (the ratio of the plasma pressure to the toroidal magnetic field pressure). Unfortunately, a toroidal plasma with an elongated cross section is subject to an axisymmetric instability [1]. It is important, therefore, to demonstrate a technique for maintaining stable plasmas with dee-shaped cross sections in current tokamak devices and to investigate their properties at high β. Experimental studies of non-circular plasmas have been performed on TOSCA, Doublet IIA, T-12 and TNT [2-6]. All of these devices are relatively small with short discharge durations. The highest elongation reported in experiments on these devices was $K \sim 1.5$. Theoretical studies have been carried out on the equilibrium and stability of non-circular plasmas which show that wall stabilization and feedback control play key roles in controlling positional instability [7-8].

In this report we will present the experimental studies of dee-shaped plasmas in Doublet III which has large plasmas and long discharge durations of almost 1 sec.

Doublet III is unique in its capability to produce plasmas with various shapes under similar conditions [9-11]. Dee-shaped plasmas have been

produced in the upper half of the Doublet III vacuum vessel. The plasma shape and position are controlled by 24 field-shaping coils with the passive and active feedback. Stable and reproducible plasmas were obtained with a surface elongation (height to width ratio) of up to 1.8. At elongations above 1.8 the plasmas became vertically unstable. No particular method was used to control the plasma current profile in this experiment.

Section 2 describes the experimental setup. Section 3 explains how the elongation was determined. Section 4 compares flux plots calculated from the MHD code with TV observations of the plasma shape. The vertical field necessary to maintain the equilibrium of dee-shaped plasmas is discussed in Section 5. In Section 6, the growth rate of the vertical instability is discussed along with a wall stabilization effect.

## 2. EXPERIMENTAL SETUP

Doublet III is a large tokamak device [12] with a major radius of 1.41 m, a minor radius of 0.45 m, and a height of 2.9 m. The vacuum vessel has an indentation in the outside wall at the midplane which results in a separation of the chamber into top and bottom lobes. Vertical position (Z) is measured from the midplane of the vacuum vessel. Most of the diagnostic instruments are installed in the upper lobe ports whose axes lie at a vertical position of Z = 0.88 m. Circular plasmas are centered on the upper port axes for the convenience of the plasma diagnostics; however, highly elongated plasmas must be positioned with their center below the port axis so as to to fit the tallest plasmas into the available volume. The plasma radius was reduced from 0.45 m to 0.41 m with the increase of the elongation. The vacuum vessel wall consists of a corrugated sheet of thin (1.5 mm) Inconel sandwiched between two flat sheets of the same material. The resistance of the vessel is 0.25 m Ω in the toroidal direction. The flux penetration time of the ohmic heating field through the vessel is roughly 1 msec.

The plasma position and shape are controlled by 24 field-shaping coils (F-coils) [13]. Each F-coil is located sufficiently close to the vacuum vessel that it may be considered to control the local flux value ($\psi_i$) at the plasma boundary. The local flux values are measured by the one-turn loop attached to the F-coil's front surface. The L/R time of each F-coil is 0.25

to 0.5 sec. The 24 F-coils and various power supplies may be connected in any combination by means of a patch panel. Figure 1 illustrates a typical connection scheme which is used to produce an elongated dee-shaped plasma. The 17 uppermost F-coils are connected in parallel to function as a conducting shell for passive control. The remaining 7 F-coils at the bottom of the vessel are left open to reduce the power supply requirements. This connection scheme is observed to eliminate the production of runaway electrons in the lower lobe of the vacuum vessel. The power supplies are indicated by square boxes in Fig. 1. They are controlled by active feedback circuits and/or preprogrammed waveform generators.

Since the shape of the vacuum vessel and the location of the F-coils, especially in the bottom section, are not designed to produce a dee-shaped plasma, five F-coils (1A, 1B, 2B, 6B, 7B) are used as the shaping coils to produce a strong pulling force from the bottom. Two F-coils (5 and 11A) are used to balance the pulling force from the top. The elongation is primarily controlled by the F1A coil through its effect on the poloidal flux values ratio $\psi_{4A}/\psi_{1A}$. Fine adjustments in the elongation are carried out with the F6B, F1B, F2B coils by changing the relative values of the poloidal magnetic flux ($\psi_i$). Each control signal is shown in Fig. 1 and the positions of many of the magnetic diagnostics are shown in Fig. 2.

The radial position $R_o$ is regulated by four outside F-coils (6A, 7A, 8A, 9A). Vertical position $Z_o$ is controlled by the upper coils, 10A and

12A. The power supplies connected to these coils are 12-pulse phase-controlled rectifier supplies which have a rise time of 4 ms and voltage output range of ±600 V. Their operational time length is 1.0 sec which is limited only by the cooling capability of the power supplies in the ohmic heating and field-shaping systems.

The plasma diagnostics used in this experiment are the following:

1. Twenty-four one-turn loops for the poloidal flux measurements on the surface of the F-coils, and 11 segmented Rogowski coils (partial Rogowski coils) to measure the distribution of the poloidal magnetic field around the minor circumference of the vacuum vessel. The former measurements are used to establish the boundary conditions in the calculation of magneto hydrodynamic (MHD) equilibria, and the latter are used to make an experimental determination of the plasma current profile. One Rogowski is used to measure the plasma current and several other simple magnetic pick up coils are used in analogue circuits to calculate plasma positions $R_o$ and $Z_o$ [14].

2. Two horizontal microwave (2 mm) interferometers at the upper-plane (Z = 0.88 m) and the midplane (Z = 0 m) are used to measure the average electron density and they are denoted $\bar{n}_e^U$ and $\bar{n}_e^M$. The average electron density along a vertical path ($\bar{n}_e^V$) is measured by the $CO_2$ laser interferometer. A useful indicator of the

plasma elongation is given by the ratio of $\overline{n}_e{}^V/\overline{n}_e{}^U$ since both densities are presented in the form of $\int n_e \, d\ell/90$ cm, where 90 cm is the approximate path length of the horizontal measurement ($\overline{n}_e{}^U$).

3. Two tangential TV camera systems are used to observe the plasma shape. They are called the upper-plane TV (Z = 88 cm) and the midplane TV (Z = 0 cm).

4. A scanning soft X-ray spectrometer and a Michelson infrared radiometer for measuring the electron temperature profile and a Thomson laser scattering system for determining the absolute electron temperature.

5. 10-channel tangential and 19-channel vertical PIN diode arrays to investigate MHD activity.

## 3. DETERMINATION OF THE PLASMA ELONGATION

The plasma shape is determined by MHD analysis using experimental magnetic data [15]. The 24 poloidal flux values ($\psi_i$) are employed as the boundary conditions in solving the Grad-Shafranov equation, and the plasma current profile is adjusted to reproduce the magnetic field distribution obtained experimentally by the partial Rogowski coils. The plasma shape derived from the calculation is shown in Fig. 2.

The plasma current profile has the form in the MHD code

$$j(R,\psi) = j_0 \left[\beta_p \frac{R}{R_p} + (1 - \beta_p)\frac{R_p}{R}\right] \left\{1 + (\gamma - 1)\left[1 - \left(\frac{\psi_M - \psi}{\psi_M - \psi_L}\right)^N\right]^M\right\} , \quad (1)$$

where R is a major radius coordinate and $R_p$ is a fixed parameter with the value of $R_p$ = 1.43 m. $\beta_p$ denotes an approximate value of the poloidal beta, and $j_0$ is the normalization factor of the plasma current. $\psi$ denotes the poloidal flux value and $\psi_M$, $\psi_L$ indicate the flux values at the magnetic axis and at the plasma surface, respectively. $\gamma$, N and M are variable parameters adjusted to reproduce the experimental data. Figure 3 illustrates how well the plasma current profile fits the partial Rogowski measurements. The fitting results are shown for three different cases of the

parameters ($\gamma$, N, M) = (A) (100, 1.0, 2.0), (B) (100, 1.3, 2.0) and (C) (60, 1.6, 2.0). The normalized internal inductances for the three cases are $\ell_i$ = (A) 1.29, (B) 1.15 and (C) 0.99. Case (B) has the smallest value of square deviation $X^2$ of the experimental and calculated partial Rogowski values [16]. Since this discharge has no sawtooth oscillation, the safety factor at the plasma center q(o) is expected to be larger than unity. Thus, case (B) is a reasonable equilibrium to describe this discharge.

From these MHD analyses, the discharge shown in Fig. 3 is determined to have an elongation of 1.8 and a triangularity of 0.3 with an approximate error of 5% and 10%, respectively.

"Elongation (K)" and "Triangularity ($\delta$)", when used without comment in this report, mean the dipole and hexapole deformations of the outermost flux contour obtained by MHD analysis. They are defined as the following,

$$K = \frac{Z_{TOP} - Z_{BOT}}{R_{OUT} - R_{IN}} \quad , \tag{2}$$

$$\delta = \frac{R_{OUT} + R_{IN} - R_{TOP} - R_{BOT}}{R_{OUT} - R_{IN}} \quad , \tag{3}$$

where the suffixes TOP, BOT, OUT, and IN mean the highest, lowest, outermost and innermost positions of the plasma surface, respectively.

Figure 4 shows the waveforms of plasma current, one-turn voltage, horizontal and vertical displacement of the plasma center from (R = 1.43 m, Z = 0.8 m), electron densities $\bar{n}_e^V$, $\bar{n}_e^U$ and $\bar{n}_e^M$, and elongation for the same discharge fitted in Fig. 3. The steady state plasma current is 530 kA. This discharge was intentionally terminated at 750 ms to measure the growth rate of the vertical instability. As described in Section 2, the plasma elongation is indicated by the density ratio $\bar{n}_e^V/\bar{n}_e^U$. During the discharge, this ratio varies between 1.6 and 1.7, which agrees with the elongation derived by MHD analysis when the path length is corrected for the triangular deformation. The increase midplane density $\bar{n}_e^M$ late in the discharge is additional evidence for large elongation.

The elongation inside the plasma, which is obtained from the MHD analysis, is constant in the central half of the plasma ($r/a < 0.5$) and increases rapidly toward the plasma surface as shown in Fig. 5. Near the magnetic axis, the maximum elongation attained was ~1.4.

## 4. COMPARISON OF MHD RESULTS WITH TV MEASUREMENTS

Plasma shape was also measured by direct observation with two TV camera systems that view the plasma cross section tangentially, one camera system was at the upper plane, the other at the midplane. In the TV pictures, the bright light from the recycling hydrogen provides an indication of the plasma surface.

The pictures in Fig. 6 show three different plasma shapes measured by the tangential upper-plane TV. For the circular plasma (a) only the inside and outside limiters appear bright. For a plasma with an elongation of 1.4 (b), both side limiters appear bright and the top limiter shows some evidence of weak recycling. For the plasma with elongation of 1.8, light appears mainly at the top limiter. These phenomena are consistent with the shapes derived from MHD analysis. The TV pictures are used during the discharge to monitor the status of the control system.

Figure 7 shows pictures of the bottom part of the plasma cross section taken with the midplane TV. An $H_\alpha$ filter was used in front of the camera to emphasize hydrogen recycling light. For the circular plasma, there is little light on the midplane. As the elongation becomes larger, the plasma becomes visible in the midplane TV. Two typical shapes are shown in Fig. 7. Shape (a) has a rather sharp corner at the inside bottom while (b) has smooth curvature. The hot core of the plasma is faint in the TV picture due to the low density of neutral hydrogen there. The sketch shown under each TV picture may assist interpretation.

## 5. EQUILIBRIUM FIELD

The decay index of the externally applied equilibrium field $n = -(R/B_Z \cdot \partial B_Z/\partial R)$ is not constant inside the plasma cross section as shown in Fig. 8. The decay index changes in value from n = -5.0 to 0.0 as a function of major radius along chord 3, the horizontal chord through the magnetic axis. The decay index values along chords 1 and 2 are different from the ones along chords 5 and 4. They are caused by the fact that the plasma shape is not up-down symmetric.

The vertical field ($B_Z$) applied by the field shaping coils can be resolved into dipole ($B_D$), quadrapole ($B_Q$), and hexapole components ($B_H$) at the magnetic axis, and expressed as a function of the major radius (R) passing through the magnetic axis [17],

$$B_Z(R) = B_D + B_Q \frac{R - R_o}{a_o} + B_H \frac{1}{2}\left(\frac{R - R_o}{a_o}\right)^2 + B^{err} \quad , \tag{4}$$

where $R_o$ and $a_o$ denote the major radius at the magnetic axis and the half width of the plasma, respectively.

Figure 9 shows the vertical field and each multipole field along chord 3 for the example of Fig. 8. $R_o$ and $a_o$ have values of 1.40 and

0.41 m, respectively. Each multipole field has the following values in this case; $B_D$ = -880 Gauss, $B_Q$ = -400 Gauss, $B_H$ = 520 Gauss. $B^{err}$ is zero at the magnetic axis and increases with the minor radius. However, maximum $B^{err}$ is less than 2% of $B_Z$, which is within the experimental error in the F-coil current measurement. $B^{err}$ is so small that the plasma shape may be considered to be correlated only to the strengths of $B_Q$ and $B_H$ [17]. Relations between the plasma shape and equilibrium field will be discussed using the decay index (n) and hexapole index [$h = (R^2/B_z) \cdot (\partial^2 B_z/\partial R^2)$]. When written at the magnetic axis using $B_D$, $B_Q$, and $B_H$, they become,

$$n = - A \frac{B_Q}{B_D} \tag{5}$$

$$h = A^2 \frac{B_H}{B_D} \tag{6}$$

where A is an aspect ratio ($R_o/a_o$).

Figure 10 shows the relation between the decay index and elongation. Closed points show the experimental data obtained using Eq. (5). These plasmas have a triangular deformation of $\delta$ = 0.25 -0.35. The solid curve is a prediction from an analytic theory assuming $\beta_p$ = 0.1, $\ell_i$ = 1.2, $R_o$ = 1.4 m, $a_o$ = 0.41 m, but without triangular deformation [18]. Both theory and experiment give dependences of the decay index on elongation which are

similar. However, the absolute values have a discrepancy of $\Delta n = -0.3 \sim -0.6$. This discrepancy is produced mainly by the triangular deformation. Figure 11 shows the triangular dependence of the decay index difference ($\Delta n = n^T - n^E$) where $n^T$ is obtained from theory and $n^E$ from experiment. The data shown in Fig. 11 includes various elongations ranging from 1.4 to 1.7. The figure indicates that the triangular deformation decreases the requirement of the quadrupole field for achieving the same elongation. This tendency is consistent with the result obtained by H. Ninomiya, et al., [17]. This fact is beneficial from the viewpoint of reducing positional instability, which is mainly correlated to the decay index value.

Figure 12 shows the relation between the triangularity of the plasma shape and the applied hexapole index [Eq. (6)]. All the data is from the same discharges as shown in Fig. 11. The scatter of data points comes from the elongation spread of K = 1.4 - 1.7. It is shown that the hexapole index has a linear relation to the triangular deformation. The plasma obtained in Doublet III does not have a simple dee-shape; it is up-down asymmetric. However, simple correlations are obtained between the parameters of the shape of the outermost plasma surface and the parameters of the equilibrium field defined at the magnetic axis. These correlations will be helpful in designing future tokamaks with dee-shaped plasmas.

## 6. WALL STABILIZATION OF THE VERTICAL INSTABILITY

An elongated plasma without a conducting shell is known to be unstable to axisymmetric modes [1]. The conducting shell that surrounds the plasma surface acts to decrease the growth rate of axisymmetric instabilities [7]. The resistive vacuum vessel in Doublet III does not provide much wall stabilization because of its short L/R decay time constant (~1 msec). However, the field shaping coils, which are located just outside the vacuum vessel and are connected in parallel with each other, act as a partial shell and produce a passive stabilization effect.

In order to evaluate the passive stabilization of the vertical instability, the following experiment was carried out. After a stable plasma was produced with active feedback control, the output voltage of the power supply for the vertical position control was turned to 0 volts The vertical position of the plasma starts to move downward and the speed increases exponentially. The plasma motion shows two different growth rates sequentially. Because the highly elongated plasma is detached from the outside limiter and there is no limiter at the bottom, the plasma is considered to keep its shape without a significant deformation by any limiters during the time when the plasma moves downward a few centimeters. Therefore, the initial growth rate is considered to be the growth rate of the vertical

instability. Figure 13 shows a typical example of the motion of the vertical position just after the active control is turned off. The initial growth rate is 78 $sec^{-1}$ with an elongation of K = 1.7.

The growth rate of the vertical instability increases with the elongation. The closed points in Fig. 14 show the growth rates of many discharges as a function of the decay index at the magnetic axis (n = -1.35 ~ -1.55). The elongation ranges from K = 1.6 to 1.8. The growth rate for plasmas with decay indices above -1.35 was so small that no measurement was carried out. The growth rate increases rapidly for n ≃ -1.5. Ideal MHD theory for a shell-less tokamak predicts a growth rate for the vertical instability of ~$10^6$ $sec^{-1}$ in an elongated plasma with a negative decay index. The difference of the experimental growth rates is caused by the passive stabilization effect of the field-shaping coil system. The eddy currents induced by the plasma motion produce a restoring force opposing the motion. This stabilization effect is estimated by calculating the induced currents through the field shaping coils, and is expressed by the denotation $n_s$ which has the same definition as Eq. (5) except that $B_Q$ is the field produced by the eddy current due to the plasma movement. The magnitude of $n_s$ depends on the plasma position and elongation. The value of $n_s$ decreases as the vertical position of the plasma center becomes low or as the elongation increases. In the present experiment, $n_s$ lies between 1.2 and 1.5. The decay time constant $\tau_s$ of this passive stabilization is about

$\tau_s$ = 350 ms. The growth rate $\gamma_G$ of the vertical motion is expressed as follows [7]:

$$\gamma_G^2 = -\tau_o^{-2}\left(n + n_s \frac{\gamma_G \tau_s}{1 + \gamma_G \tau_s}\right) , \tag{7}$$

where $\tau_o$ denotes the ideal MHD time constant. The solid line in Fig. 14 indicates the growth rate derived from Eq. (7) with $n_s$ = 1.5, $\tau_s$ = 350 msec, $\tau_o$ = 1 μsec. The experimental result for the growth rate is explained by this numerical calculation. This indicates that the stabilization effect is primarily due to the F-coils although it is also expected from other structures. Active feedback control completely stabilizes the positional instability of plasmas with elongtions of less than 1.8, which are obtained in this measurement.

## 7. CONCLUSION

Stable plasmas with elongations over the entire range from 1.0 to 1.8 are produced in the upper half of Doublet III. The discharge lasts about 1 sec with a current flattop of ~0.5 sec. Highly elongated plasmas are achieved by increasing the height of the cross section, which slightly decreases the width.

Up-down asymmetry appears in the plasma cross section because the machine is not designed for symmetric dee-shaped plasmas. Almost all of the stable dee-shaped plasmas obtained have a triangular deformation of ~0.3. The triangularity relates linearly to the hexapole field index. The triangular deformation of the cross section tends to reduce the value of the decay index relative to that required for an ellipse of the same elongation. This suggests that a dee-shaped plasma is more positionally stable than an elliptical plasma.

The field-shaping coils, which are connected in parallel and are located close to the plasma surface, play a large part in stabilizing positional instability. The measured growth rates of the vertical instability without active feedback control are consistent with the rates calculated from the passive stabilization of the field-shaping coils.

Active feedback control completely stabilizes the positional instability of the plasmas with elongations of less than 1.8.

ACKNOWLEDGEMENT

The authors would like to express their sincere gratitude to Dr. T. Ohkawa and the staff of the General Atomic Company for their great hospitality. This experiment was carried out with the fine support of the diagnostics group under Dr. R. Fisher and the machine operation group under Dr. R. Callis. The authors would like to express their appreciation to Dr. J. Luxon for his careful reading of this manuscript. The authors would also like to thank Drs. M. Yoshikawa and S. Mori and the staff at the Japan Atomic Energy Research Institute for their continuing encouragement throughout this work.

Active feedback control completely stabilizes the positional instability of the plasmas with elongations of less than 1.8.

ACKNOWLEDGEMENT

The authors would like to express their sincere gratitude to Dr. T. Ohkawa and the staff of the General Atomic Company for their great hospitality. This experiment was carried out with the fine support of the diagnostics group under Dr. R. Fisher and the machine operation group under Dr. R. Callis. The authors would like to express their appreciation to Dr. J. Luxon for his careful reading of this manuscript. The authors would also like to thank Drs. M. Yoshikawa and S. Mori and the staff at the Japan Atomic Energy Research Institute for their continuing encouragement throughout this work.

## REFERENCES

[1] YOSHIKAWA, S., Phys. Fluids 7 (1964) 278.

[2] ROBINSON, D. C., WOOTTON, A. J., Nucl. Fusion 18 (1978) 1555.

[3] FISHER, R. K., ADCOCK, S. J., BAUR, J. F., BROOKS, N. H., DeBOO, J. C., FREEMAN, R. L., GUSS, W. C., HELTON, F. J., HSIEH, C. L., JENSEN, T. H., LIETZKE, A. F., LOHR, J. M., MAHDAVI, M. A., MATSUDA, K., MOELLER, C. P., OHKAWA, T., OHYABU, N., PRAGER, S. C., RAWLS, J. M., TAMANO, T., VANEK, V., WANG, T. S., Phys. Rev. Lett. 39 (1977) 622.

[4] BORTINIKOV, A. V., BREVNOV, N. N., GERASIMOV, S. N., ZHUKOVSKII, V. G., PERGAMENT, V. I., KHIMCHENKO, L. N., in Controlled Fusion and Plasma Physics (Proc. 8th Europ. Conf. Prague, 1977) 41.

[5] TOYAMA, H., MAKISHIMA, K., KARNEKO, H., NOGUCHI, M., YOSHIKAWA, S., Phys. Rev. Lett. 37 (1976) 18.

[6] LIPSHULTZ, V., PRAGER, S. C., TODD, A. M. M., DELUCIA, J., Nucl. Fusion 20 (1980) 683.

[7] FUKUYAMA, A., SEKI, S., MOMOTA, H., ITATANI, R., Jpn. J. Appl. Phys. 14 (1975) 871.

[8] HAAS, F. A., PAPALOIZOUS, J. C. B., Nucl. Fusion 17 (1977) 721.

[9] JAERI TEAM, Nucl. Fusion 20 (1980) 1455.

[10] NAGAMI, M., SHIMADA, M., YOKOMIZO, H., SEKI, S., KONOSHIMA, S., FUJISAWA, N., OHARA, Y., SUGAWARA, T., BROOKS, N. H., GROEBNER, R., SERAYDARIAN, R., KITSUNEZAKI, A., Nucl. Fusion 20 (1980) 1325.

[11] WESLEY, J. C., et al., in Plasma Physics and Controlled Nuclear Fusion Research (Proc. 8th Int. Conf. Brussels, 1980) paper IAEA-CN-38/A-3.

[12] CALLIS, R. W., General Atomic Company Report GA-A13996 (1976).

[13] STAMBAUGH, R., ADCOCK, S., CALLIS, R., DEGRASSIE, J., LUXON, J., ROCK, P., WESLEY, J., SEKI, S., SHIMADA, M., YOKOMIZO, H., in Fusion Technology (11th Symp. Oxford, 1980) 1011.

[14] YOKOMIZO, H., SEKI, S., SHIMADA, M., NAGAMI, M., KONOSHIMA, S., FUJISAWA, N., OHARA, Y., IOKI, K., KITSUNEZAKI, A., General Atomic Company Report GA-A15931 (1981).

[15] McCLAIN, F. W., BROWN, B. B., General Atomic Company Report GA-A14490 (1977).

[16] LUXON, J. L., BROWN, B. B., General Atomic Company GA-A15970 (1981).

[17] NINOMIYA, H., SHINYA, K., KAMEARI, A., in Engineering Problems of Fusion Research (Proc. 8th Symp. San Francisco, 1979) 75.

[18] SUZUKI, Y., NINOMIYA, H., OGATA, A., KAMEARI, A., AIKAWA, H., Jpn. J. Appl. Phys. 16 (1977) 2237.

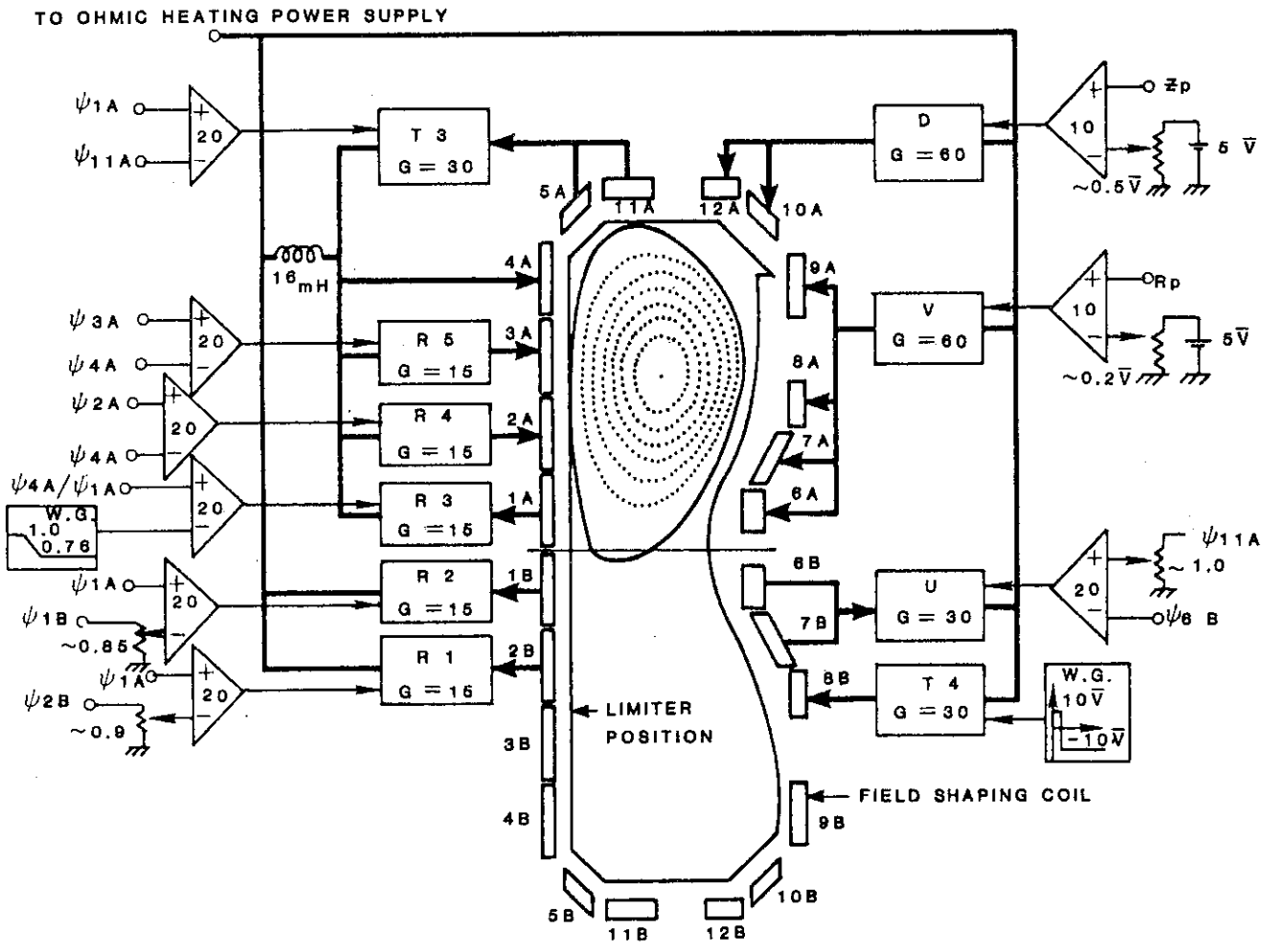


FIG. 1 A control schematic for dee-shaped plasmas. Voltage gains are indicated on the power supplies and differential amplifiers. Feedback signals are shown as inputs for differential amplifiers. The 17 field-shaping coils are connected in parallel with each other and connected to an ohmic heating power supply. Big lines show the current flow with arrows indicating the direction. D, V and R denote thyrister power supplies with (60 Hz, ± 600 V, + 14 kA), (60 Hz, ± 600 V, + 21 kA), (60 Hz, + 150 V, + 3 kA) capabilities, respectively. T and U are chopper power supplies with (1 kHz, ± 300 V, + 3 kA), (1 kHz, ± 250 V, ± 2.5 kA) capabilities.

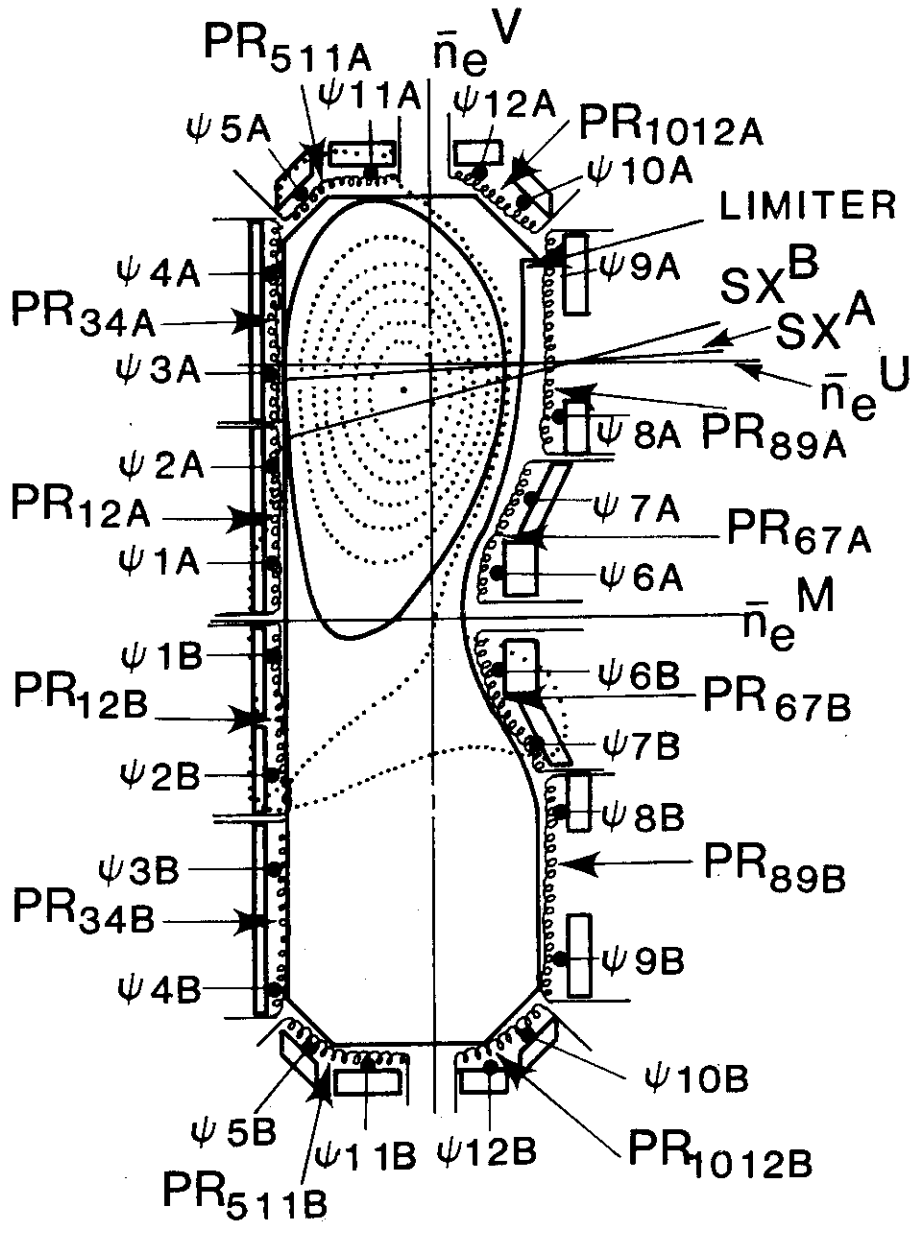


FIG. 2 Magnetic diagnostic locations and a plasma shape with an elongation of 1.8. $\bar{n}_e^V$ and $\bar{n}_e^U$, $\bar{n}_e^M$ indicate the density measuring paths of a $CO_2$ laser and 2 mm microwave interferometers. $SX^A$ and $SX^B$ show the viewing paths of the soft X-ray PIN diodes. PR denotes 12 segmented Rogowski coils, and $\psi$ denotes one-turn loops. $PR_{12A}$ was not used.

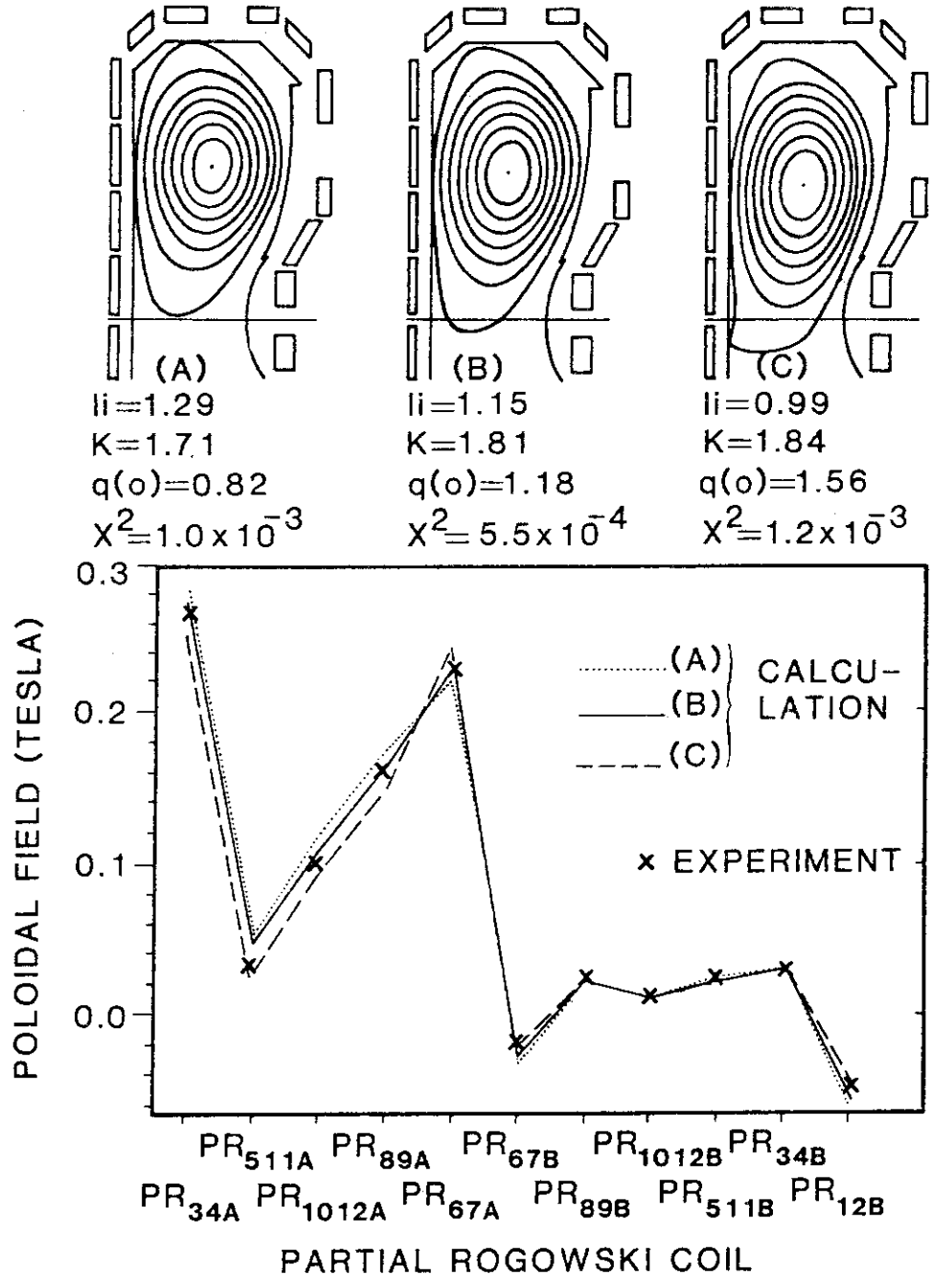


FIG. 3 Three plasma shapes produced by MHD analysis of a discharge using different current profiles. $\ell_i$, K, q(o), $X^2$ denote the normalized internal inductance, the surface elongation, the safety factor at the magnetic axis and the square deviation of the poloidal field strength. The cross points show the measured poloidal field strength.

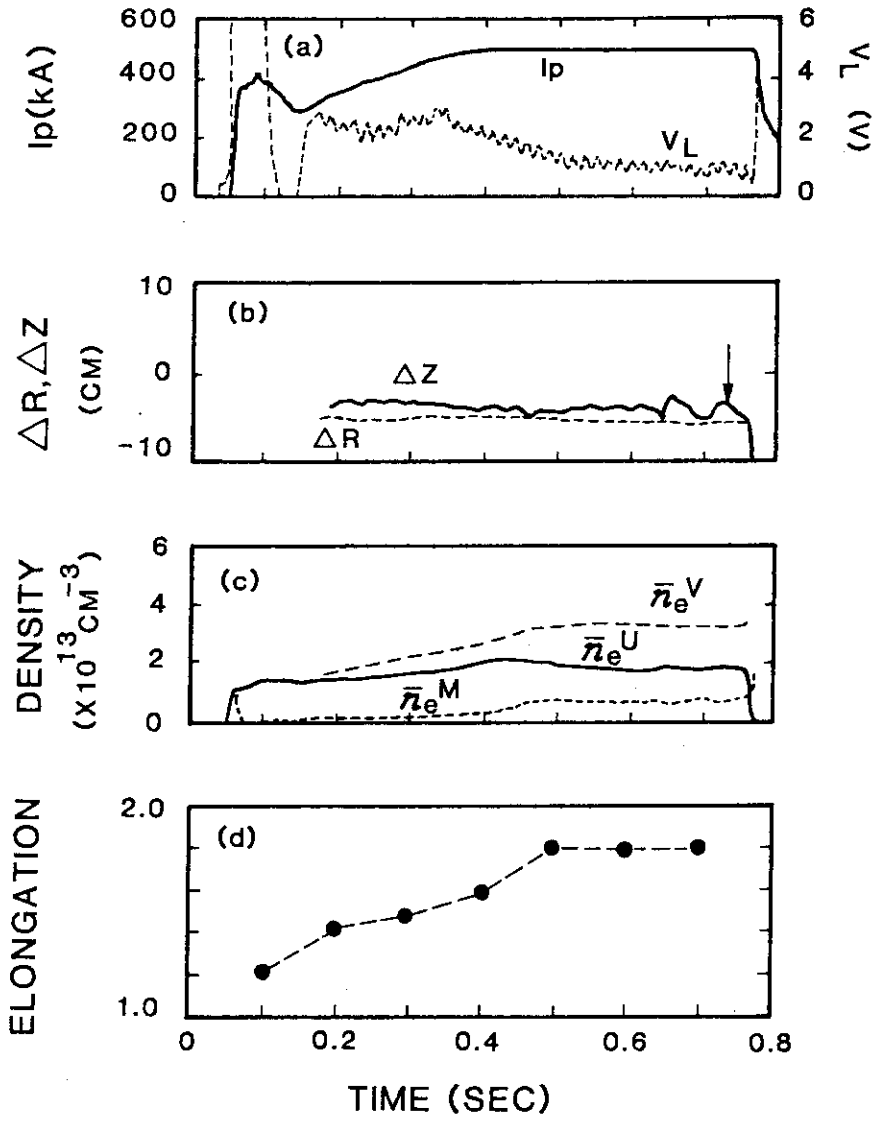


FIG. 4 Wave forms of a typical discharge: (a) plasma current and one-turn voltage, (b) radial and vertical position, (c) average electron densities in vertical ($\bar{n}_e^V$) and horizontal ($\bar{n}_e^U$, $\bar{n}_e^M$) paths, (d) elongation derived from MHD analysis. The vertical position control is turned off at the time indcated by the arrow in order to investigate positional instability. The discharge is the same one as shown in Fig. 3.

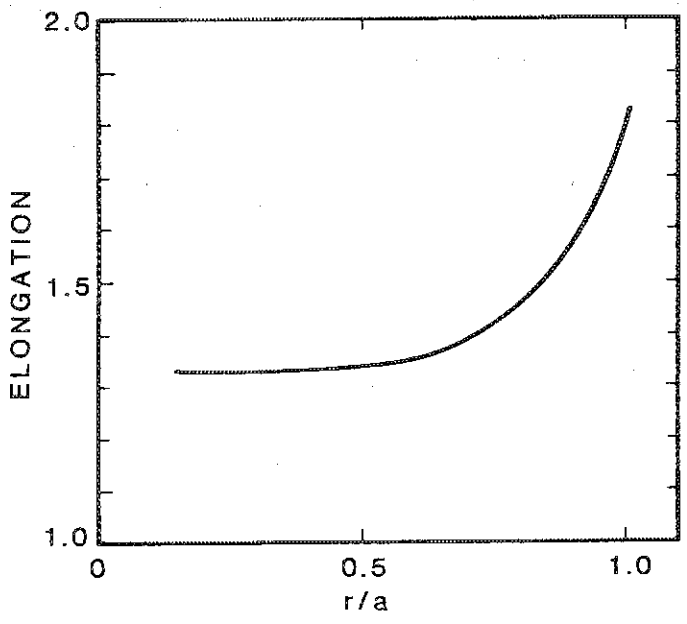


FIG. 5 Elongation of the flux surface inside the plasma. This discharge is the same one as shown in Fig. 3.

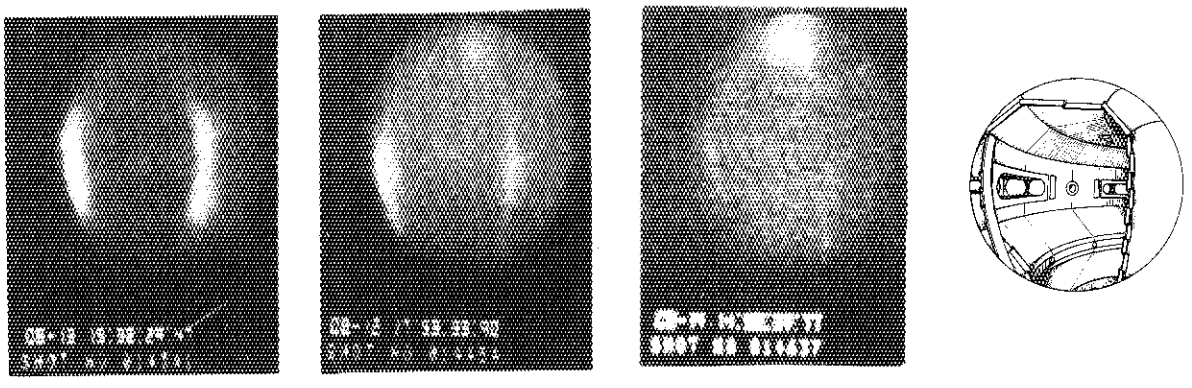

(a) (b) (c) (d)

K = 1.05 K = 1.35 K = 1.8

$I_p$ = 530 kA $I_p$ = 530 kA $I_p$ = 530 kA

$\bar{n}_e = 4.5 \times 10^{13} cm^{-3}$ $\bar{n}_e = 3 \times 10^{13} cm^{-3}$ $\bar{n}_e = 2.5 \times 10^{13} cm^{-3}$

Fig. 6

FIG. 6 The TV pictures tangentially viewing the upper lobe of the vacuum vessel. Three shapes have elongations of K = 1.05, 1.35 and 1.8.

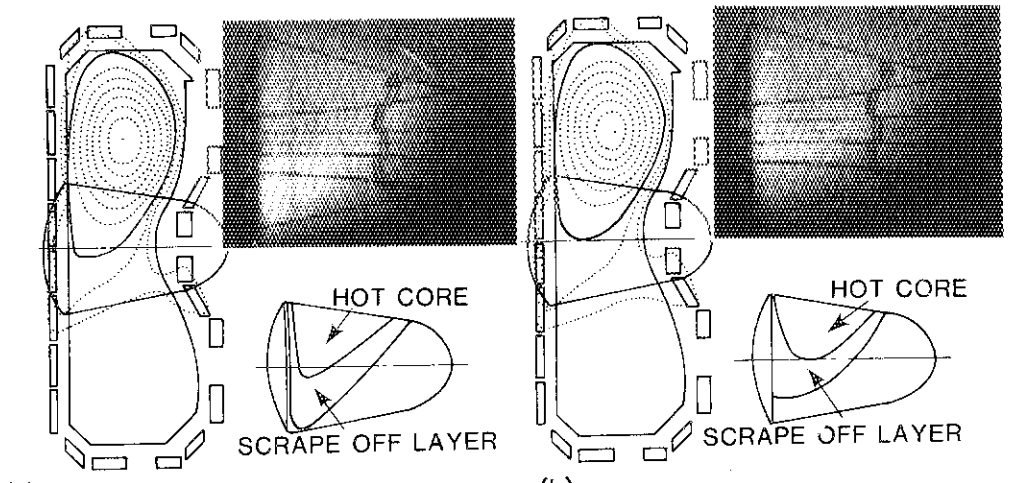


(a) K = 1.85
Ip = 530 kA
$\bar{n}_e = 2.2 \times 10^{13}$ cm$^{-3}$

(b) K = 1.75
Ip = 530 kA
$\bar{n}_e = 2.1 \times 10^{13}$ cm$^{-3}$

Fig. 7

FIG. 7 The TV pictures tangentially viewing the bottom part of the dee-shaped plasma. The equilibrium shapes obtained from MHD analysis are also shown for comparison.

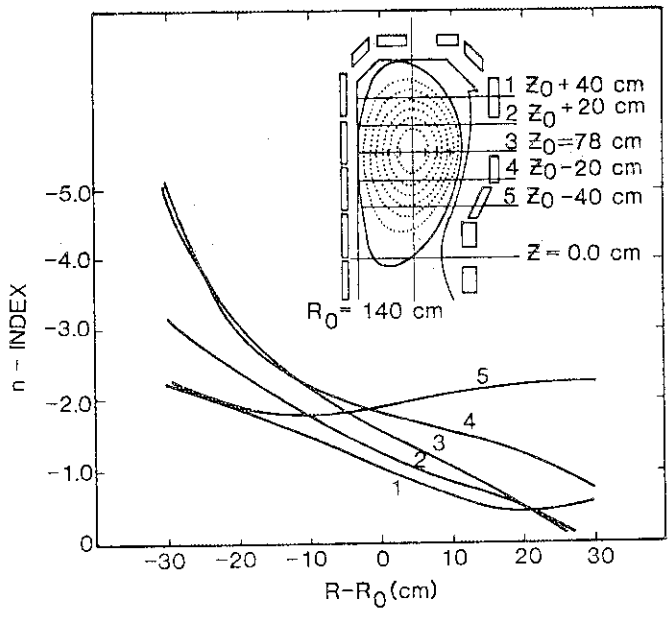


FIG. 8 Decay index [$n = -(R/B_Z \cdot \partial B_Z/\partial R)$] of the externally applied equilibrium field inside the plasma cross section calculated using the F-coil currents. (This discharge is the same one as shown in Fig. 2.) $Z_o$ (78 cm) is the vertical position of the magnetic axis. R is the horizontal distance from the magnetic axis $R_o$.

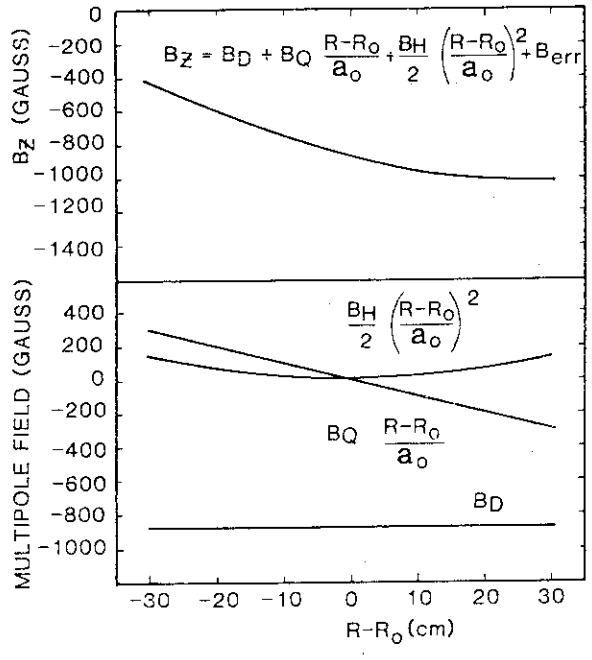


FIG. 9 Experimentally applied vertical ($B_Z$) and dipole ($B_D$), quadrapole $\{B_Q [(R - R_o)/a_o]\}$, and hexapole $\{B_H/2 [(R - R_o)/a_o]^2\}$ field components on chord 3 as shown in Fig. 8.

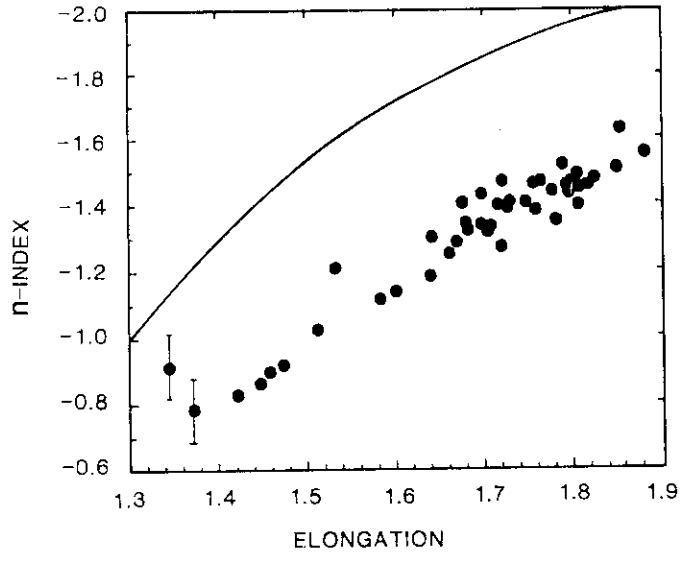


FIG. 10 The relation between decay index and elongation. Closed points show experimental results. The solid curve indicates a theoretical prediction assuming $\beta_p = 0.1$, $\ell_i = 1.2$, $R_o = 1.4$ m, $a_o = 0.41$ m. The triangularity of these data spreads from 0.25 to 0.35. Typical experimental errors are shown by bars.

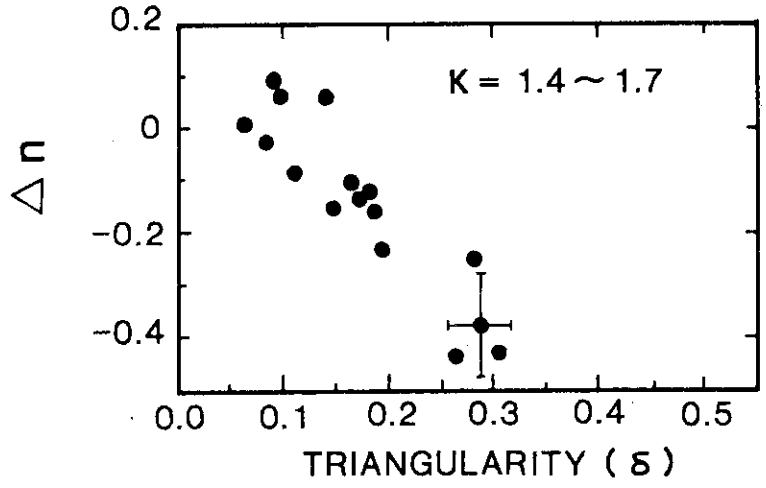


FIG. 11 Triangularity effect upon the discrepancy $\Delta n = n^T - n^E$ between theoretical predictions ($n^T$) and experimental results ($n^E$) on the decay index. The elongation for these data ranges from 1.4 to 1.7. A typical experimental error is shown by the cross.

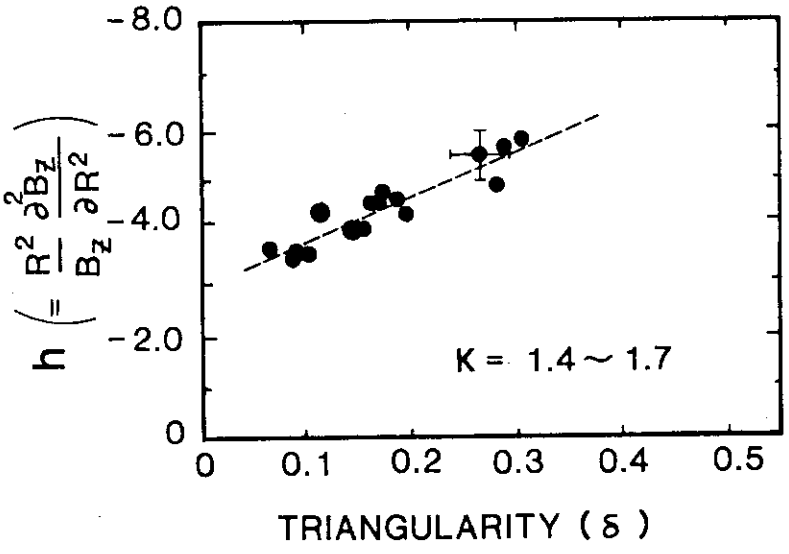


FIG. 12 Relation between the hexapole index [$h = (R^2/B_Z \cdot \partial^2 B_Z/\partial R^2)$] and the triangularity. Data are for the same shots shown in Fig. 11.

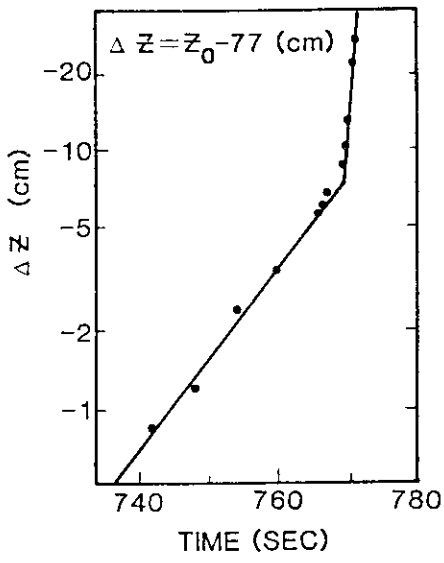


FIG. 13 Vertical displacement of the plasma center just after the active control of the vertical position is turned off. The elongation is 1.73, $I_p$ = 550 kA, $B_T$ = 20 kG. The growth rates are $\gamma_G$ = 78 $sec^{-1}$ and 710 $sec^{-1}$.

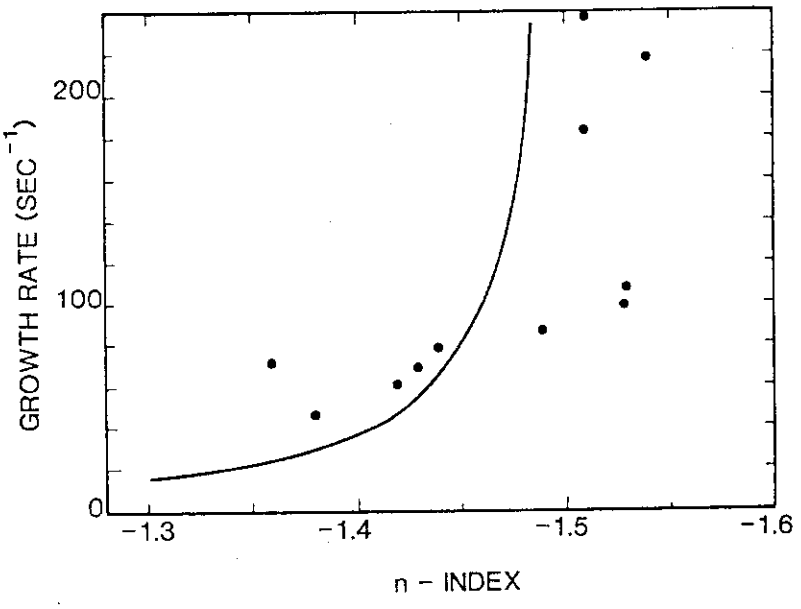


FIG. 14 The relation of the growth rate with the decay index. The closed circles show the initial growth rate just after the active control of the vertical position is turned off. The solid line indicates the theoretical prediction using $n_s$ = 1.5, $\tau_s$ = 350 ms, and $\tau_o$ = 1 μs to characterize the stabilizing effect from the field-shaping coils.